TU Delft

Delft University of Technology

Document Version
Final published version

Licence
Dutch Copyright Act (Article 25fa)

Citation (APA)
Liu, Y., Tian, Y., Kang, F., Wagemaker, M., Li, B., & Chen, G. (2025). Stabilized P–F Bond for Sustainable and Ultralong Life High-Energy Lithium Batteries. *Advanced Functional Materials*, *36*(9), Article e19229. https://doi.org/10.1002/adfm.202519229

Important note
To cite this publication, please use the final published version (if applicable).
Please check the document version above.

Copyright
In case the licence states “Dutch Copyright Act (Article 25fa)”, this publication was made available Green Open Access via the TU Delft Institutional Repository pursuant to Dutch Copyright Act (Article 25fa, the Taverne amendment). This provision does not affect copyright ownership.
Unless copyright is transferred by contract or statute, it remains with the copyright holder.

Sharing and reuse
Other than for strictly personal use, it is not permitted to download, forward or distribute the text or part of it, without the consent of the author(s) and/or copyright holder(s), unless the work is under an open content license such as Creative Commons.

Takedown policy
Please contact us and provide details if you believe this document breaches copyrights.
We will remove access to the work immediately and investigate your claim.

This work is downloaded from Delft University of Technology.

Check for updates

ADVANCED FUNCTIONAL MATERIALS
www.afm-journal.de

Stabilized P—F Bond for Sustainable and Ultralong Life High-Energy Lithium Batteries

Yuanming Liu, Yao Tian, Feiyu Kang, Marnix Wagemaker, Baohua Li,* and Guohua Chen**

The instability of P—F bond-based electrolyte (PFE) under ambient conditions presents one of the biggest challenges for the production, usage, and recycling of lithium (Li) batteries. It increases the cost of battery production, decreases battery service life, and harms human health and environmental sustainability during the use of batteries. Here a stabilized P—F bond electrolyte (SPFE) is reported, which can effectively prevent the side-reactions in PFE at ambient conditions. The SPFE, which is pristine, containing ultra-high content of water (10 000 ppm or 10 g L^{-1}), can support the 2 Ah Li-ion pouch cell (200 Wh kg^{-1}) cycling 400 times with 90.2% of its capacity retained. The mostly dry room-free (DRF) production of commercial Li-ion (2Ah, 200 Wh kg^{-1}) and anode-free (AF) Li metal pouch cell (2 Ah, 410 Wh kg^{-1}) also demonstrated excellent cycling stability with the SPFE. Moreover, the SPFE enables AF Li-metal batteries (AFLMBs) to retain 54.1% of their charged capacity even after 180 days of open circuit storage. By intrinsically safeguarding PFE from hydrolysis, the present SPFE would have a broad impact on future battery technology, simplifying battery production, extending battery service life, and safeguarding battery recyclability.

1. Introduction

Since the introduction of P—F bond (Specifically, $LiPF_6$) containing electrolytes (PFE)[1] in the 1990s along with lithium (Li) layered metal oxide as cathode and graphite as anode,[2] lithium ion batteries (LIBs) have become the dominant technology for energy storage systems accounting for a more than US$ 100 billion manufacturing market nowadays. Up to now, PFE is still indispensable in Li battery technology for its balanced properties such as excellent electrochemical stability, suitable Li-ion conductivity, wide operation temperature, and versatile compatibility with various electrodes.

The sensitivity to humidity presents a key challenge to PFE in ambient conditions, necessitating expensive fabrication in dry rooms with a very low dew point (<−40 °C (≈20 ppm)), which accounts for more than 25% of the cost required for the whole line of battery production.[3] Furthermore, the hydrolysis of P—F bond during the long-term cycling process of batteries will still hinder the performance of LIBs significantly[4] and potentially initiate battery explosion.[5] For the next generation high energy Li metal batteries (LMBs), the unstable P—F bond can also induce severe corrosion of the Li metal anode (LMA), causing a minimum capacity decay of 2% to 3% per day.[6] Moreover, the unstable P—F bond also poses a great challenge for human safety and environmental sustainability during the recycling process of the used LIBs.[7]

The susceptibility of the P—F bond to hydrolysis, however, is inevitable by the trace amounts of moisture in battery components such as both anode and cathode electrodes, separator, and package film. The hydrolysis of the P—F bond produces hydrogen fluoride (HF) and various acidic species such as HPO_2F_2, H_2PO_3F, inducing cracks in the solid-electrolyte interphase (SEI), dissolution of transition metal (TM) ions in layered metal oxide cathodes, and decomposition of electrolyte solvent.[8] In addition, the degraded P—F bond would catalyze the ring opening of cyclic carbonates to form the polymeric species having a carbonate motif,[9] which degrades the electrolyte by turning the color from transparent into brown, and eventually black. The amount of the as-formed acidic species is as high as 5.4 to 53.7 grams (g) in one electric vehicle battery pack,[10] which makes the processing of the used batteries challenging because of toxicity to humans and the environment. Various strategies have been

Y. Liu, Y. Tian, F. Kang, B. Li
Guangdong Provincial Key Laboratory of Thermal Management Engineering & Materials
Tsinghua Shenzhen International Graduate School
Tsinghua University
Shenzhen 518055, China
E-mail: libh@sz.tsinghua.edu.cn
Y. Liu, G. Chen
School of Energy and Environment
City University of Hong Kong
Hong Kong, China
E-mail: kechengh@ust.hk
M. Wagemaker
Department of Radiation Science and Technology
Delft University of Technology
Delft 2629JB, The Netherlands
E-mail: m.wagemaker@tudelft.nl
G. Chen
Department of Chemical and Biological Engineering
The Hong Kong University of Science and Technology
Clear Water Bay, Kowloon, Hong Kong SAR, China

The ORCID identification number(s) for the author(s) of this article can be found under https://doi.org/10.1002/adfm.202519229

DOI: 10.1002/adfm.202519229

 © 2025 Wiley-VCH GmbH

proposed to stabilize P—F bond in electrolytes, including the promotion of $LiPF_6$ dissociation,[11] the addition of PF_5 scavenger,[12] the HF scavenger,[9b,13] and also the humidity reducer.[13–14] However, until now, the humidity-tolerance of PFE is still below 1000 ppm (or 1 g L^{-1}), although the battery electrodes are fabricated under ambient and dry room free conditions, experiencing water content of over 2000 ppm.[3b,15] Thus, it becomes obvious that for a stable battery production, one can either complete the manufacture in a dry room with ultralow dewpoint or formulate a PFE with a tolerance of water content over 2000 ppm. The latter option is highly desirable, although extremely difficult.

Here we report a stabilized P—F bond-based electrolyte (SPFE) that could eliminate the water induced side-reactions in PFE effectively. By introducing NO_3^-, the PF_5 from $LiPF_6$-degradtion can be largely absorbed, which thoroughly decreases the PF_5-catalyzed solvent decomposition. In the meantime, the H_2O inside SPFE can be well contained without degrading the P—F bond by the absorption of NO_3^- and the Nef reaction produced aldehydes. Moreover, the consumption of H_2O by the Nef reaction can effectively decrease the water content in SPFE. As a consequence, the SPFE after 60 days of ambient storage exhibits no decomposition of the P—F bond and solvent. A coin LIBs ($LiNi_{0.6}Mn_{0.2}Co_{0.2}O_2$-graphite) with this electrolyte presents more than 500 stable cycles. In addition, for the SPFE with pristine 10 000 ppm of water and after 15 days of ambient-storage, it could still support the 2 Ah (200 Wh kg^{-1}) Li-ion pouch cell with 90.2% of its discharge capacity retained after 400 cycles. The SPFE electrolyte can also enable the mostly dry room-free (DRF) production of 2 Ah Li-ion and anode-free (AF) Li metal pouch cell with excellent cycling stability. Moreover, the SPFE restrains the corrosion of charged high energy AF Li metal battery (AFLMB) effectively, delivering an excellent cycling stability and retaining 54.1% of its charged capacity even after 180 days of calendar aging.

2. Preparation of Stabilized P—F Bond-Based Electrolyte (SPFE)

The bare electrolyte (1M $LiPF_6$ in EC/DEC (1/1, v/v) with 10 wt.% FEC, which is suitable for both Li ion batteries (LIBs) and Li metal batteries (LMBs)), bare electrolyte with Li metal, bare electrolyte with $LiNO_3$ particles and bare electrolyte with both Li metal and $LiNO_3$ particles were prepared and stored in ambient conditions first, and they are denoted as Am, Am-Li, Am-L and Am-Li-L, respectively. These well-prepared electrolytes were placed in sealed glass vials and then stored under ambient conditions with a temperature ranging from 15 to 30 °C and relative humidity (RH) varying from 40% to 70%. After 60 days, the Am-L-60d and Am-Li-L-60d electrolytes remain transparent, while the Am-60d electrolyte has gradually turned brown (Figure S1, Supporting Information). After 90 days, the Am-90d electrolyte becomes dark brown in distinct contrast with the colorless Am-L-90d and Am-Li-L-90d electrolytes. For the electrolyte stored in an argon (Ar) atmosphere, 90 days of storage can also make the Ar-90d electrolyte become faint brown, while this is totally not the case for other electrolytes (Figure S2, Supporting Information).

3. Component and Performance of SPFE

Solution nuclear magnetic resonance (NMR) is used to characterize the components of ambient- and argon-stored electrolytes. As shown in Figure S3 (Supporting Information), the ^1H NMR spectra of Am-60d and Am-Li-60d electrolytes show the evident presence of the defluorinated FEC, but this cannot be seen for the Am-L-60d and Am-Li-L-60d electrolytes. In addition, for the Li-L electrolytes (Am-Li-L-60d and Ar-Li-L-60d) stored in ambient or argon environment, aldehydes (RCHO) are found (**Figure 1a**; Figure S4a, Supporting Information). The formation of aldehydes is the result of the Nef reaction involving water consumption.[16] The ^{31}P and ^{19}F NMR spectra of the ambient- and argon-stored electrolytes show that the decompositions in Am or Ar electrolyte were effectively impeded in Am-L or Ar-L electrolyte, whereas they were impeded more efficiently in Am-Li-L or Ar-Li-L electrolyte (Figure 1b–d; Figure S4b–d, Supporting Information). For both Am-Li-L-60d and Ar-Li-L-60d electrolytes, the P—F bond degradation is almost eliminated during the 60 days storage. The comparison between the ^1H NMR spectra for the ambient- (Figure 1a) and argon- (Figure S4a, Supporting Information) stored electrolytes shows that only the coexistence of Li metal and $LiNO_3$ in PFE can produce aldehydes (RCHO).

The time-of-flight secondary ion mass spectrometry (TOF-SIMS) depth profiling of several secondary ion fragments on the Li metal surface in Am-Li-L-60d electrolyte is shown in Figure 1e,f, which displays the existence of H^-, O^-, F^-, LiF^-, $C_3H_6^-$, $C_2H_5O^-$, and $C_2HNO_2^-$. The presence of O^- and LiF^- should be derived from the $LiNO_3$ and $LiPF_6$ or FEC degradation, respectively. However, the $C_2HNO_2^-$ must originate from the reduction of $LiNO_3$ and carbonate solvent at the Li metal surface, which initiates the Nef reaction in the presence of H_2O or H^+.[16] After 60 or 90 days of ambient storage, the water content for the Am electrolyte is only 33 or 54.4 ppm (Figure 1g), a consequence of hydrolysis that leads to the brown color, in agreement with the literature reports.[8a,13–14,17] The addition of Li metal in the Am electrolyte could eliminate the side reactions to some extent, resulting in a water content of 65.8 ppm (107.3 ppm after 90 days). In contrast, the Am-L and Am-Li-L electrolytes have water content of 357.1 ppm (360.3 ppm after 90 days) and 225.5 (283.8 after 90 days) ppm, respectively, showing the suppressed detrimental hydrolysis.

The Am-Li-L-60d electrolyte supports the coin-type LIB ($LiNi_{0.6}Mn_{0.2}Co_{0.2}O_2$ (NMC622) | graphite (G)) to cycle stably over 500 times with a capacity retention of 59%, much better than that of Am-60d electrolyte with a capacity retention of 13% after only 100 cycles (Figure 1h–j; Figures S5 and S6a, b, Supporting Information). It is worth noting that the Am-L-60d electrolyte allows coin LIB to cycle stably during the initial 100 cycles. The difference in performance between Am-L-60d and Am-Li-L-60d electrolytes is supposed to be the consequence of the Nef reaction with aldehydes produced, which decreases the water content and subsequently suppresses the production of harmful species. Anode-free LMB (AFLMB, NMC622 | Cu) were assembled to further evaluate the electrochemical performance of the ambient-stored electrolytes. The Am-Li-L electrolyte is found to withstand calendar aging of the charged AFLMB (to 4.3 V). After 10 days of calendar aging of the charged AFLMB, the cell with Am-Li-L-60d electrolyte maintains 89% of its charge capacity, while the

© 2025 Wiley-VCH GmbH

16163028, 2026, 9, Downloaded from https://advanced.onlinelibrary.wiley.com/doi/10.1002/adfm.202519229 by Tu Delft, Wiley Online Library on [09/02/2026]. See the Terms and Conditions (https://onlinelibrary.wiley.com/terms-and-conditions) on Wiley Online Library for rules of use; OA articles are governed by the applicable Creative Commons License

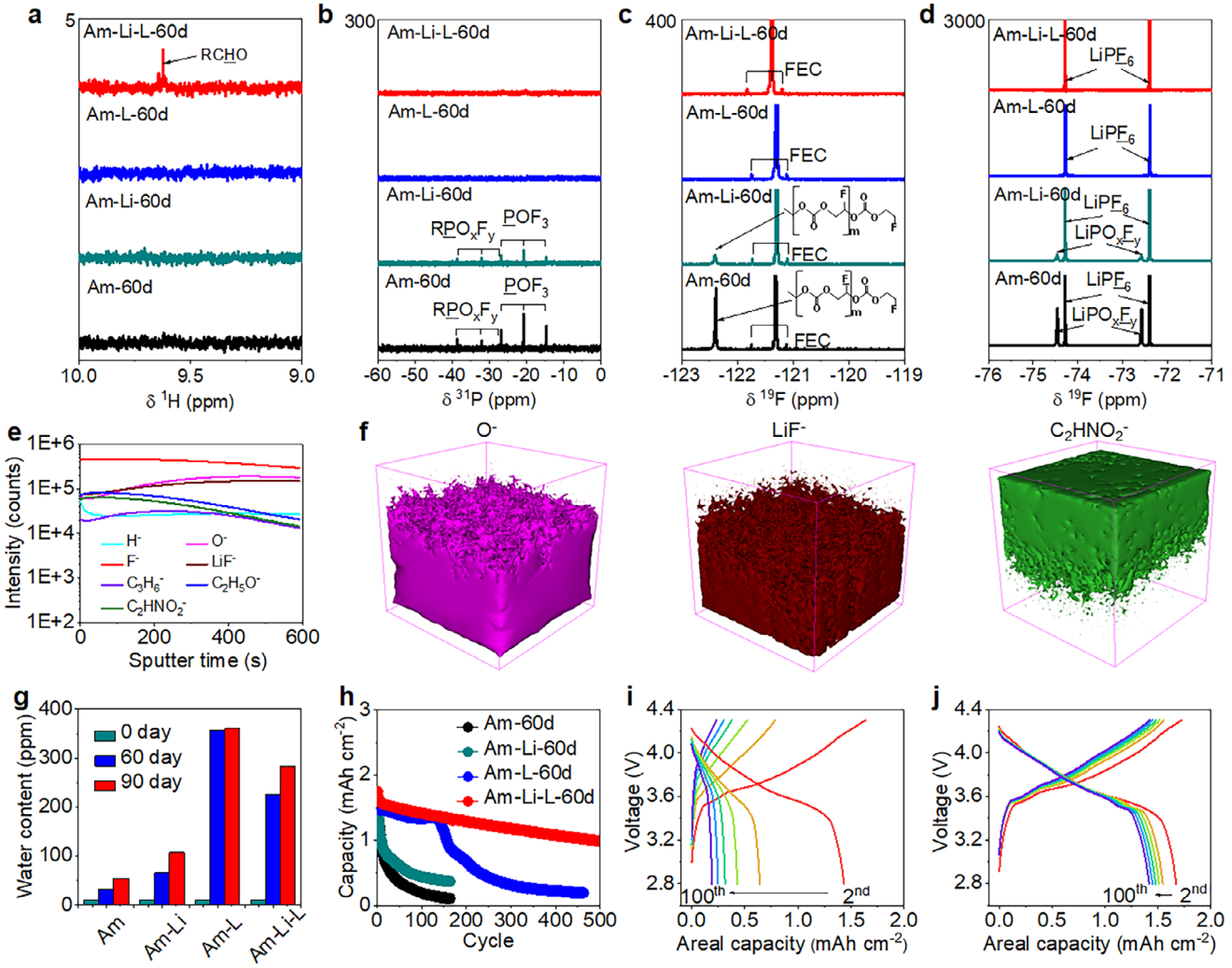

Figure 1. Preparation of stabilized P—F bond-based electrolyte (SPFE). a, b) ^{1}H and ^{31}P solution NMR spectra of ambient (Am)-stored PFE electrolyte after 60 days (Bare electrolyte (Am-60d), bare electrolyte with Li foil (Am-Li-60d), bare electrolyte with $LiNO_3$ particles (Am-L-60d) and bare electrolyte with both Li foil and $LiNO_3$ particles (Am-Li-L-60d)), respectively. c, d) ^{19}F solution NMR spectra of Am, Am-Li-60d, Am-L-60d and Am-Li-L-60d samples. e) Time-of-flight secondary ion mass spectrometry (TOF-SIMS) depth profiling of several secondary ion fragments on the Li metal surface of Am-Li-L-60d sample. f) TOF-SIMS 3D reconstruction of the sputtered volume on the surface of Li metal of Am-Li-L-60d sample. g) Water content of different ambient-stored electrolytes. h) Cycling performance of the $LiNi_{0.6}Mn_{0.2}Co_{0.2}O_2$ (NMC622) | graphite (G) coin cell with ambient-stored electrolytes after 60 days. i, j) Voltage-capacity profile of NMC622 | G coin cell using Am-60d and Am-Li-L-60d electrolyte, respectively.

Am-60d electrolyte records a capacity retention of 44.4% only (Figures S6c, d and S7, Supporting Information). Even after 90 days of storage, the Am-Li-L-90d and Ar-Li-L-90d electrolytes can still exhibit excellent aging and cycling performances of AFLMBs (Figure S8, Supporting Information).

4. Mechanism of SPFE

As shown in **Figure** 2a, in general, the PFE electrolyte, the reassociation of Li^+ and PF_6^- would lead to the formation of PF_5 and LiF.[4a,9b,c,18] Then, the produced PF_5 would be subject to hydrolysis in the presence of water and produce POF_3 and HF. The POF_3 could further hydrolyze to produce various acidic species and HF. However, in SPFE, the NO_3^- and carbonate solvent will form $C_2HNO_2^-$ at the surface of Li metal, as evidenced by the TOF-SIMS results in Figure 1e,f, which will further react with H_2O or H^+ in SPFE and produce aldehyde species and N_2O (Figure 2b, as evidenced by the NMR results in Figure 1a; Figure S4a, Supporting Information).[16] This is helpful in decreasing the contents of water and HF in SPFE, thus inhibiting the harmful degradation significantly. Such a result can also be testified by the pH tests shown in Figure S1 (Supporting Information), where the Am-Li-L electrolytes exhibit the lowest acidity compared with others.

To reveal the interactions between representative molecules in SPFE, a density functional theory calculation was conducted (Figure S9, Supporting Information). The calculated Gibbs free energy for the interactions between different molecules is shown in Figure 2c. Typically, the $LiPF_6$ degraded product, PF_5, is inclined to absorb H_2O (Binding energy $\Delta E = -39.7$ kJ mol^{-1}), forming POF_3 and HF. The interaction between POF_3 and H_2O

© 2025 Wiley-VCH GmbH

16163028, 2026, 9, Downloaded from https://advanced.onlinelibrary.wiley.com/doi/10.1002/adfm.202519229 by Tu Delft, Wiley Online Library on [09/02/2026]. See the Terms and Conditions (https://onlinelibrary.wiley.com/terms-and-conditions) on Wiley Online Library for rules of use; OA articles are governed by the applicable Creative Commons License

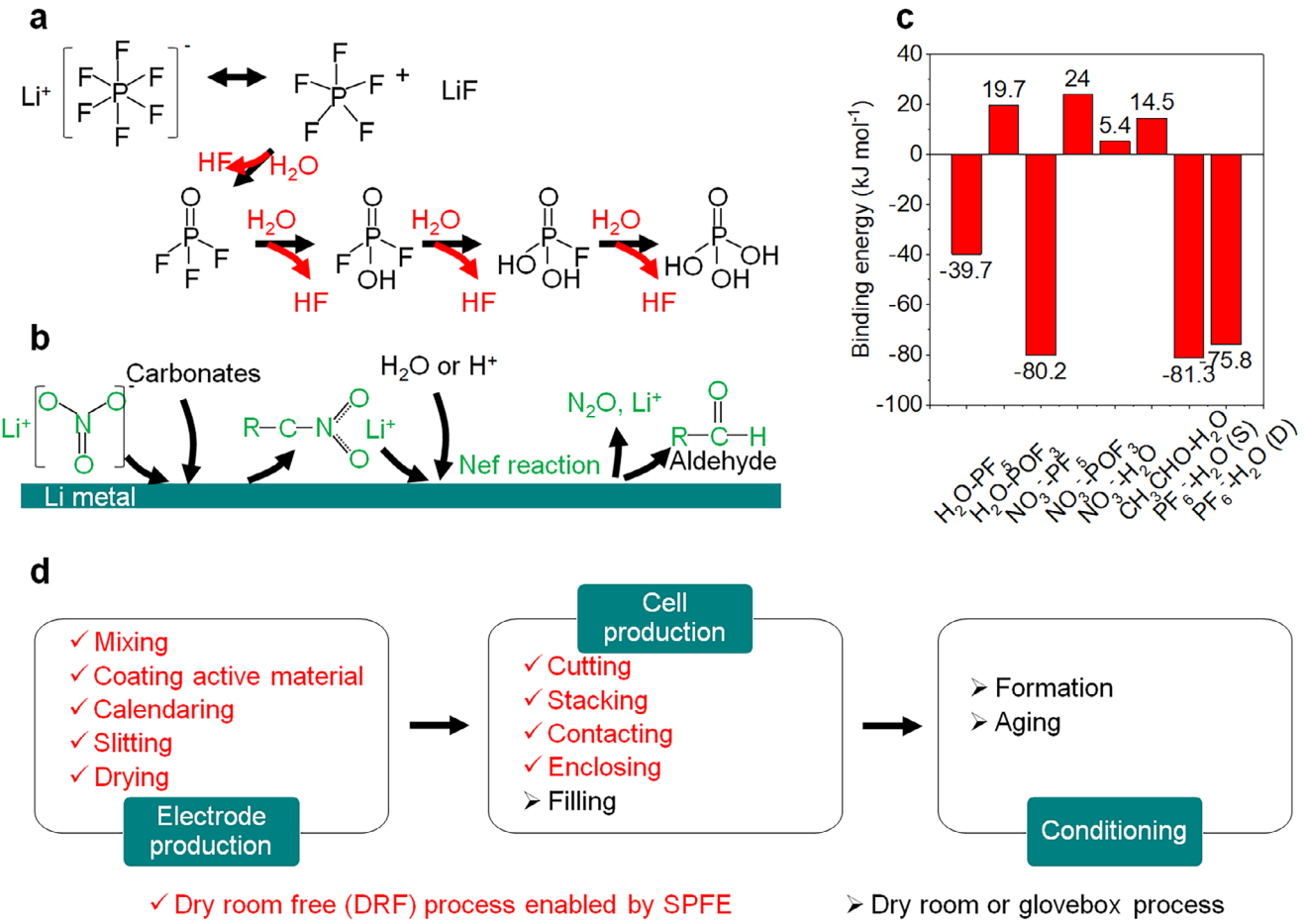

Figure 2. Mechanism and function of SPFE. a) Schematic showing the degradation routes of $LiPF_6$ salt in PFE. b) Schematic showing the reaction routes on Li metal surface in SPFE. c) Calculated Gibbs free energy for the interactions between different molecules in SPFE. d) SPFE enabled mostly dry room free (DRF) production of commercialized lithium batteries.[22]

is not that strong ($\Delta E = 19.7$ kJ mol^{-1}), with external energy required for their reaction to proceed. However, with the addition of $LiNO_3$, the NO_3^- ions can absorb PF_5 spontaneously $\Delta E = -80.2$ kJ mol^{-1}). The value of binding energy for the absorption between NO_3^- and PF_5 is two times that between H_2O and PF_5, indicating that the hydrolysis of PF_5 would be largely restrained in SPFE if there are sufficient NO_3^-. This simulation result agrees well with the reported research that the addition of $LiNO_3$ can only stabilize $LiPF_6$-based electrolyte effectively and achieve a humidity tolerance of 1000 ppm.[19] The interaction between NO_3^- and POF_3 is weaker than that between H_2O and POF_3. However, the binding energy values of NO_3^- and the as-formed aldehydes, for example, the CH_3CHO derived from the ethyl group of DEC) absorption with water are relatively smaller than that between POF_3 and H_2O, which further inhibits the hydrolysis of POF_3. It is also worth noting that the interactions between PF_6^- anions and H_2O molecules (−81.3 kJ mol^{-1} between PF_6^- anion and single hydrogen atom of H_2O (Figure S9c, Supporting Information) and −75.8 kJ mol^{-1} between PF_6^- anion and double hydrogen atom of H_2O (Figure S9d, Supporting Information)) are comparable to the interactions between PF_5 and NO_3^-, which further show that the only existence of $LiNO_3$ in $LiPF_6$-based electrolyte cannot restrain its hydrolysis effectively when the content of H_2O is very high (for example, >2000 ppm). These calculations are based on the FEC dielectric constant[20] of $\varepsilon_{FEC} = 78.4$, while it has also been reported[21] to exceed a value of 100. Although we believe that the dielectric constant of FEC should be smaller than EC (89.8), and that the $\varepsilon_{FEC} = 78.4$ is a realistic value (Note S1 and Figure S10, Supporting Information), DFT calculations are also performed with ε_{FEC} assumed to be 102.9. Except for the interaction between NO_3^- and PF_5 resulting in a positive absorption energy, the interactions between NO_3^- and H_2O and between CH_3CHO and H_2O are preferable compared to that between POF_3 toward H_2O, supporting the aforementioned results (Figure S11, Supporting Information).

5. Ambient Stored SPFE Containing 10000 ppm H_2O

There are three major processes for battery production, including electrode production, cell production, and conditioning (Figure 2d).[22] Generally, all these processes should be carried out in a dry room with a very low dew point to avoid moisture contamination of the electrolyte. However, if the PFE could

© 2025 Wiley-VCH GmbH

16163028, 2026, 9, Downloaded from https://advanced.onlinelibrary.wiley.com/doi/10.1002/adfm.202519229 by Tu Delft, Wiley Online Library on [09/02/2026]. See the Terms and Conditions (https://onlinelibrary.wiley.com/terms-and-conditions) on Wiley Online Library for rules of use; OA articles are governed by the applicable Creative Commons License

tolerate the ambient humidity (a few thousand ppm),[3b] then the operations marked in red in Figure 2d can be carried out under ambient conditions, significantly decreasing the cost of battery production.

To test the tolerance of SPFE to moisture, it was subjected to a more severe condition where 1wt.% of H_2O (10000 ppm) was added to the electrolyte. As expected, the SPFE electrolyte is effective in suppressing the harmful decomposition reactions in PFE, as shown in **Figure 3a–d** and Figure S12 (Supporting Information). After 15 days of ambient storage, the water content of H_2O-Am-15d electrolyte decreased to 110.3 ppm, demonstrating the serious decomposition of PFE, while this has been strongly suppressed in the H_2O-Am-L-15d (6238.9 ppm) and H_2O-Am-Li-L-15d (3987.6 ppm) electrolytes. The NMR results for the water containing electrolyte after 15 days of ambient storage show that, when the water content increases to 10 000 ppm, there is also a clearly existence of POF_3 and HF_2^- for the ambient-stored electrolyte with $LiNO_3$ only (Figure S13, Supporting Information), which is contrast to the undegraded electrolyte protected by both $LiNO_3$ and Li metal. Even when the temperature is increased to 40 °C, the electrolyte containing both $LiNO_3$ and Li metal is still more efficient than the electrolyte containing $LiNO_3$ only in protecting the PFE electrolyte (Figure S14, Supporting Information). For the pouch type LIB cells (Figure S15, Supporting Information) with newly prepared water-containing electrolytes and ambient-stored water-containing electrolytes, the gassing phenomena for the pouch cells injected with the H_2O-0d (Figure S16b, Supporting Information), H_2O-L-0d (Figure S16c, Supporting Information), H_2O-Am-L-15d (Figure S17c, Supporting Information; Figure 3g) and H_2O-Am-Li-L-15d (Figure S17d, Supporting Information; Figure 3h) electrolytes can be clearly seen, while this cannot be observed for the pouch cells injected with the newly prepared clean electrolyte (Figure S16a, Supporting Information), H_2O-Am-15d (Figure S17a, Supporting Information; Figure 3e) and H_2O-Am-Li-15d electrolytes (Figure S17b, Supporting Information; Figure 3f), demonstrating the strong moisture tolerance of our SPFE electrolyte.

For the newly prepared water-containing electrolytes, the H_2O-L-0d electrolyte could support the 2 Ah (200 Wh kg^{-1}) Li-ion pouch cell maintain a discharge capacity of 1.2 Ah and energy efficiency of 85.7% after 400 cycles, while the cell with H_2O-0d electrolyte exhibits a discharge capacity of 1.3 Ah and energy efficiency of 84.8% after only 100 cycles (Figure S18, Supporting Information). After ambient storage, the electrochemical performance for the cell with Am-H_2O-15d electrolyte (Figure 3i,j,l, with less than 0.5 Ah capacity after only 50 cycles and energy efficiency lower than 85%) is even worse than the cell with H_2O-0d electrolyte, ascertaining the significant decomposition of H_2O-0d electrolyte during ambient storage. Whereas, the H_2O-Am-Li-L-15d electrolyte could maintain the Li-ion pouch cell running at 95% (1.93 Ah) of its designated capacity (2Ah) at the first cycle of 0.5 C, and still delivering a high capacity of 1.74 Ah (90.2% capacity retention) and energy efficiency of 92% even after 400 cycles (Figure 3i,j,m), which is almost equivalent to that of newly prepared clean electrolyte (with a capacity retention of 94% and energy efficiency of 95% after 400 cycles, Figure S18, Supporting Information). The addition of Li metal (H_2O-Am-Li-15d) or $LiNO_3$ particles (H_2O-Am-L-15d) independently can also increase the capacity retention as well as the energy efficiency of LIBs to some extent; the electrolyte that contains both of them shows the obvious advantage of SPFE electrolyte. Since the density of $LiNO_3$ and Li metal is ≈2.38 and 0.534 g cm^{-3}, respectively, the $LiNO_3$ particles will precipitate at the bottom of SPFE electrolyte, whereas the Li metal will float on its surface during the long-term aging process, because the density of SPFE is ≈1 g cm^{-3}. And therefore, there is no existence of $LiNO_3$ particles in the above pouch cells. The water tolerance for the present SPFE is one magnitude or more higher than published results,[3a,23] and the reported cell capacity as well as the capacity retention are also significantly higher than most of them (Figure 3k; Table S1, Supporting Information).

To demonstrate the effectiveness of the present SPFE toward industry-scale production of LIBs, Li-ion pouch cells (2Ah) were further produced under mostly dry room-free conditions. Typically, apart from the filling of electrolyte and the conditioning of cells, all the other processes were carried out in ambient conditions with a temperature range from 25 to 28 °C and humidity range from 55% to 75%, the red font processes described in Figure 2d. The cell with SPFE electrolyte can still deliver a high capacity of 1.88 Ah and energy efficiency of 93.1% even after being cycled 500 times at 0.5 C, while the cell with PFE electrolyte can only maintain a capacity of 1.36 Ah and energy efficiency of 88.2% after only 400 cycles (Figure 3n,o; Figure S19, Supporting Information).

6. SPFE for Decreased Corrosion in AFLMBs

For the next-generation high energy density Li metal batteries (LMBs), the corrosion of Li metal anode (LMA) is a very serious problem during the cycling and calendar aging process,[6,24] especially for the anode-free LMBs (AFLMBs), which have a very limited Li source for the high energy density of LMBs. Therefore, we further tested the SPFE in AFLMBs for suppression of the P—F bond decomposition induced corrosion. According to the former results, the SPFE is formed by the co-existence of Li metal and $LiNO_3$ in PFE. The difference between LIBs and AFLMBs is that, during the charging process of AFLMBs, Li metal would be formed accordingly. Therefore, only $LiNO_3$ was added as electrolyte additive in PFE by using the PP/$LiNO_3$/PP separator[25] (PP: polypropylene) as SPFE electrolyte in AFLMBs. Although many research works have reported the increased cycling stabilities of LMBs[25–26] or even the LMBs with water containing PFE[19] when $LiNO_3$ was used as electrolyte additive in PFE, the corrosion resistance of $LiNO_3$-added PFE has been rarely explored. Especially for the interplay between Li metal and $LiNO_3$ in stabilizing PFE in practical batteries, which has never been reported.

First, AFLMBs with PP/PP separator (PFE) or PP/$LiNO_3$/PP separator (SPFE) were charged to 4.3 V, and then it was followed by remaining to OCV for 2 or 30 days. Due to the larger dimension of Cu foil (16 mm in diameter) compared to the cathode (12 mm in diameter), an obvious Cu border can be observed for the extracted anodes of charged AFLMBs (Figure S20, Supporting Information). The Cu border for the PFE-4.3 V sample exhibits a distinct black color compared to the unchanged Cu border from the cells with SPFE electrolyte (Figure S20a, c, Supporting Information). After 2 days of calendar aging at OCV of charged AFLMBs (to 4.3 V), the black color of Cu border of PFE-4.3V-2d sample deepens, and the morphology for the deposited Li

© 2025 Wiley-VCH GmbH

16163028, 2026, 9, Downloaded from https://advanced.onlinelibrary.wiley.com/doi/10.1002/adfm.202519229 by Tu Delft, Wiley Online Library on [09/02/2026]. See the Terms and Conditions (https://onlinelibrary.wiley.com/terms-and-conditions) on Wiley Online Library for rules of use; OA articles are governed by the applicable Creative Commons License

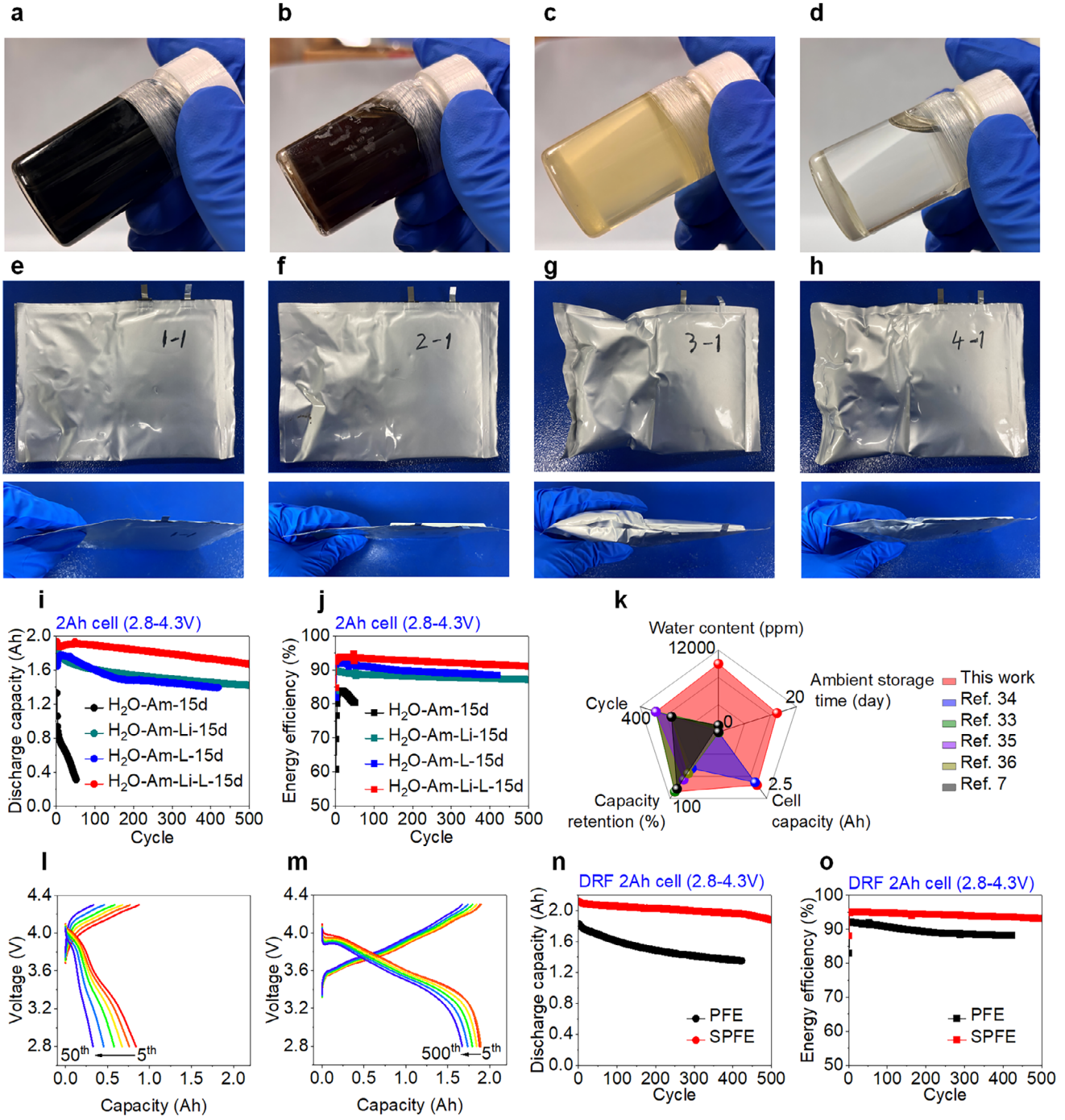

Figure 3. Performance of LIBs with SPFE. Digital photos for the electrolyte containing 10 000 ppm of water and after ambient-storage of 15 days: a) bare electrolyte (H_2O-Am-15d); b) bare electrolyte with Li foil (H_2O-Am-Li-15d); c) bare electrolyte with $LiNO_3$ particles (H_2O-Am-L-15d); d) bare electrolyte with both Li foil and $LiNO_3$ particles (H_2O-Am-Li-L-15d). e, f, g, h) Front and side digital images of the activated pouch cell which was injected with the ambient-stored electrolyte of H_2O-Am-15d, H_2O-Am-Li-15d, H_2O-Am-L-15d and H_2O-Am-Li-L-15d, respectively. i, j) Cycling performance and energy efficiency of NMC811-Graphtie pouch cells (2Ah, 200 Wh kg^{-1}) injected with ambient-stored and water-containing electrolytes, respectively. k) Comparisons for the cycling performance of LIBs with the present SPFE and with other reported stabilized PFEs. l, m) Voltage-capacity profile of NMC811-Graphtie pouch cell with H_2O-Am-15d and H_2O-Am-Li-L-15d electrolyte, respectively. n, o) Cycling performance and energy efficiency of NMC811-Graphtie pouch cells (2Ah, 200 Wh kg^{-1}) which were fabricated under the mostly dry room free (DRF) conditions and injected with PFE and SPFE electrolytes, respectively.

© 2025 Wiley-VCH GmbH

16163028, 2026, 9, Downloaded from https://advanced.onlinelibrary.wiley.com/doi/10.1002/adfm.202519229 by Tu Delft, Wiley Online Library on [09/02/2026]. See the Terms and Conditions (https://onlinelibrary.wiley.com/terms-and-conditions) on Wiley Online Library for rules of use; OA articles are governed by the applicable Creative Commons License

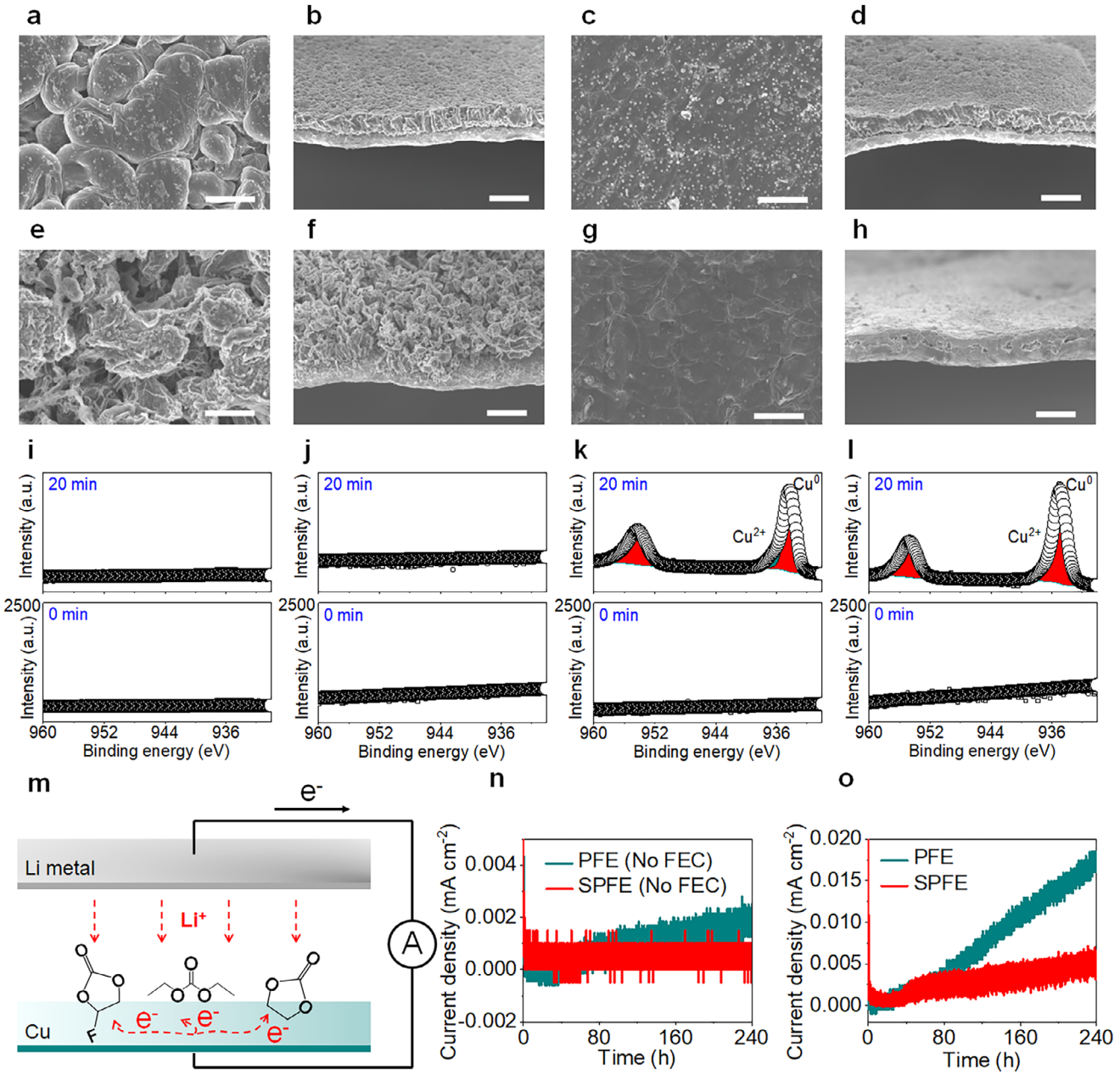

Figure 4. SPFE suppressed corrosion of Li metal anode in high energy AFLMBs. SEM images of charged anode (to 4.3 V) in AFLMB: a, b) with PFE electrolyte (PFE-4.3V); c, d) with SPFE electrolyte (SPFE-4.3V). SEM images of aged anode (to 4.3 V and after 2 days storage at open circuit voltage (OCV)) in AFLMB (to 4.3 V) after 2 days with e, f) PFE electrolyte (PFE-4.3V-2d) and g, h) SPFE electrolyte (SPFE-4.3V-2d). i, j) XPS Cu2p depth spectra on the Cu part of charged anode (to 4.3 V) and aged anode (to 4.3 V and after 2 days storage at OCV) in AFLMB with PFE electrolyte, respectively. k, l) XPS Cu2p depth spectra on the Cu part of charged anode (to 4.3 V) and aged anode (to 4.3 V and after 2 days storage at OCV) in AFLMB with SPFE electrolyte, respectively. m) Schematic illustration of the half-cell to test the galvanic corrosion of Li metal anode. n, o) Galvanic corrosion current for the cell with FEC-free electrolyte (PFE (No FEC) and SPFE (No FEC)) and FEC-containing electrolyte (PFE and SPFE), respectively.

metal changes from densely packed to mossy like porous fibers (Figure S20b, Supporting Information; **Figure 4a,b,e,f**). In contrast, the color of Cu border of SPFE-4.3V-2d sample remains unchanged, and the Li metal still has a densely packed structure (Figure S20d, Supporting Information; Figure 4c,d,g,h). Even after 30 days of calendar aging, the SPFE-4.3V-30d sample still retains a large amount of deposited Li metal, showing little reaction by-products on both the anode and separator (Figure S20h–j, Supporting Information), while the deposited Li metal for the PFE-4.3V-30d sample has been completely corroded, showing large amounts of reaction by-products on both the anode and separator (Figure S20e–g, Supporting Information). For the electrochemical impedance spectroscopy (EIS) of the charged AFLMBs with PFE and SPFE electrolyte, a significant increase in impedance

© 2025 Wiley-VCH GmbH

16163028, 2026, 9, Downloaded from https://advanced.onlinelibrary.wiley.com/doi/10.1002/adfm.202519229 by Tu Delft, Wiley Online Library on [09/02/2026]. See the Terms and Conditions (https://onlinelibrary.wiley.com/terms-and-conditions) on Wiley Online Library for rules of use; OA articles are governed by the applicable Creative Commons License

for the battery with PFE electrolyte can be clearly observed after 10 days of calendar aging process (Figure S21a, Supporting Information), while the cell with SPFE electrolyte shows little change before and after 10 days of calendar aging process (Figure S21b, Supporting Information).

X-ray photoelectron spectroscopy (XPS) was utilized to characterize the disassembled anode in AFLMBs. For the disassembled anodes in AFLMBs with PFE, the signals of the Cu element cannot be captured at the Cu border of both the charged anode (PFE-4.3V, Figure 4i) and the aged anode (PFE-4.3V-2d, Figure 4j), even after 20 min of depth profiling. However, clear Cu signals for both the disassembled anodes in the charged AFLMBs (SPFE-4.3V, Figure 4k) and the aged AFLMBs (SPFE-4.3V-2d, Figure 4l) have been captured, showing the strongly suppressed galvanic corrosion between Li metal and Cu current collector. This can also be testified by the much-reduced galvanic corrosion current between Li metal and Cu foil in Li | Cu half cells with SPFE electrolyte (Figure 4m–o). For the aged anodes in charged AFLMBs after 30 days, the C1s spectra on Li metal of PFE-4.3V-30d sample is rich in inner C—C groups, showing serious decomposition of carbonate solvent. However, the C—C groups of SPFE-4.3V-30d sample are mainly located at the surface (Figure S22, Supporting Information), reflecting less decomposition of electrolyte. In addition, the O1s spectra on both the Li metal and Cu border of SPFE-4.3V-30d sample are abundant in Li_2O (Figure S23, Supporting Information), which should result from the $LiNO_3$ decomposition, supporting the cycling stability of AFLMBs.[27] Moreover, as shown in Figure S24 (Supporting Information), the formations of $Li_xPF_yO_z$ and LiF species (F1s spectra) on both the Li metal and Cu border have been largely suppressed in AFLMBs with SPFE electrolyte. This agrees well with the P2p spectra (Figure S25, Supporting Information), where the formation of $Li_xPF_yO_z$, Li_3PO_4, and Li_3P species has also been significantly decreased on both the anode and cathode. Because $LiPF_6$ is the only source for phosphorus species, and because both $LiPF_6$ and FEC are the only sources for fluorine species, the above XPS results demonstrate the restrained decomposition of $LiPF_6$ and FEC in SPFE. Severe dissolutions of manganese (Mn) ions can also be observed in the PFE sample (Figure S26a, c, Supporting Information). The dissolution of Mn ions in the layered oxide cathode and their redeposition on the anode surface is harmful for battery operation to their reactivity toward SEI and electrolyte, which would result in severe capacity fading and safety concerns.[4c,5,28] However, such phenomena have been totally prevented in AFLMBs with SPFE (Figure S26b,d, Supporting Information). The XPS analysis clearly shows that the decomposition of PFE electrolyte induced corrosion on both anode and cathode, but the cross-talk of dissolved transition metal (TM) ions has been totally suppressed in AFLMBs with SPFE.

To further demonstrate the SPFE suppressed corrosion in AFLMBs, all the anode, separator, and cathode (Figure S27, Supporting Information), the only anode (Figure S28, Supporting Information), and the only cathode (Figure S29, Supporting Information) were disassembled from the charged AFLMBs (to 4.3V) with PFE electrolyte, and then they were soaked in PFE electrolyte (1M $LiPF_6$ in EC/DEC (1/1, v/v) with 10wt.% FEC, denoted as PFE) or PFE electrolyte with $LiNO_3$ particles (denoted as SPFE) and further submitted to ambient storage. The PFE electrolyte with all the disassembled-anode, separator, and cathode changes to reddish-brown after 14 days, while the SPFE electrolyte remains transparent (Figure S27, Supporting Information). The color of the reddish-brown should originate from the dissolution of transition metal ions of the layered oxide cathode, because after 60 days of ambient storage, the PFE electrolyte with disassembled anode only still remains colorless (Figure S28, Supporting Information), whereas the PFE electrolyte with disassembled cathode only changes to be reddish-brown (Figure S29, Supporting Information). It is worth noting that the SPFE electrolyte with disassembled-anode or cathode still remains colorless even after 60 days, demonstrating the effectiveness of SPFE to suppress the dissolution of transition metal ions, consistent with the XPS results.

7. SPFE for Ultralong Life AFLMBs

To investigate the capacity retention and cycle life under realistic cycling conditions, we fabricated AFLMBs with PFE or SPFE electrolyte for long-term corrosion tests. First, a one-day intermittent aging test was employed for AFLMB with high loading NMC622 or single crystalline $LiNi_{0.8}Mn_{0.1}Co_{0.1}O_2$ (SCNMC811) cathode, with the battery charged to 4.3 V and held at this OCV for one day (24 h) followed by a discharge to 2.8 V, as shown in **Figure 5**a,b and Figure S30,S31 (Supporting Information). The average Coulombic efficiency (ACE) for the SPFE sample is 97.2% and 98.1% for the NMC622 and SCNMC811 cathode, respectively, which is superior to that of the PFE sample (89.8% and 93% for the NMC622 and the SCNMC811 cathode, respectively). In addition, the same one-day intermittent aging test was also applied to Li | Cu half cells with an ACE for SPFE of 97% and PFE of 95.8% found, as shown in Figure 5c and Figure S32 (Supporting Information). The comparisons for the ACE between these AFLMBs and Li | Cu half cells show that for PFE samples, the serious dissolution of transition metal ions and the as-induced side reactions would decrease the ACE value from 95.8% (for Li | Cu half cells) to 89.8% and 93% for AFLMBs with NMC622 and SCNMC811 cathode, respectively. However, the ACE for the AFLMBs with SPFE electrolyte (97.2% for NMC622 and 98.1% for SCNMC811) is higher than that of Li | Cu half cells with the same configurations (97%), demonstrating that not only the side reactions associated with the dissolution of transition metal ions were totally avoided, the galvanic and chemical corrosion of Li metal anode has also been suppressed, agreeing well with the galvanic test results in Figure 4m–o.

The battery with SPFE shows a capacity retention of 90.4% instead of 25.2% for that with PFE electrolyte after 30 days of calendar aging of the charged AFLMBs (Figure 5d–f; Figure S33, Supporting Information). The one with PFE worked for only 36 cycles, while that with SPFE operated with a high capacity-retention of 81.8% for the 2nd aging test and a longer cycling life of over 90 times. Both the charge protocol and cathode chemistry have little impact on the aging and subsequent cycling performance of AFLMBs (Figure S34, Supporting Information). Even for the cell that was initially injected with PFE electrolyte, replacing the PFE electrolyte with SPFE electrolyte at the charged state of AFLMBs can also increase the cycling and aging performances of AFLMBs significantly (Figure S35, Supporting Information). The most impressive result is that the AFLMBs with SPFE electrolyte could retain 54.1% of their charged capacity after

© 2025 Wiley-VCH GmbH

16163028, 2026, 9, Downloaded from https://advanced.onlinelibrary.wiley.com/doi/10.1002/adfm.202519229 by Tu Delft, Wiley Online Library on [09/02/2026]. See the Terms and Conditions (https://onlinelibrary.wiley.com/terms-and-conditions) on Wiley Online Library for rules of use; OA articles are governed by the applicable Creative Commons License

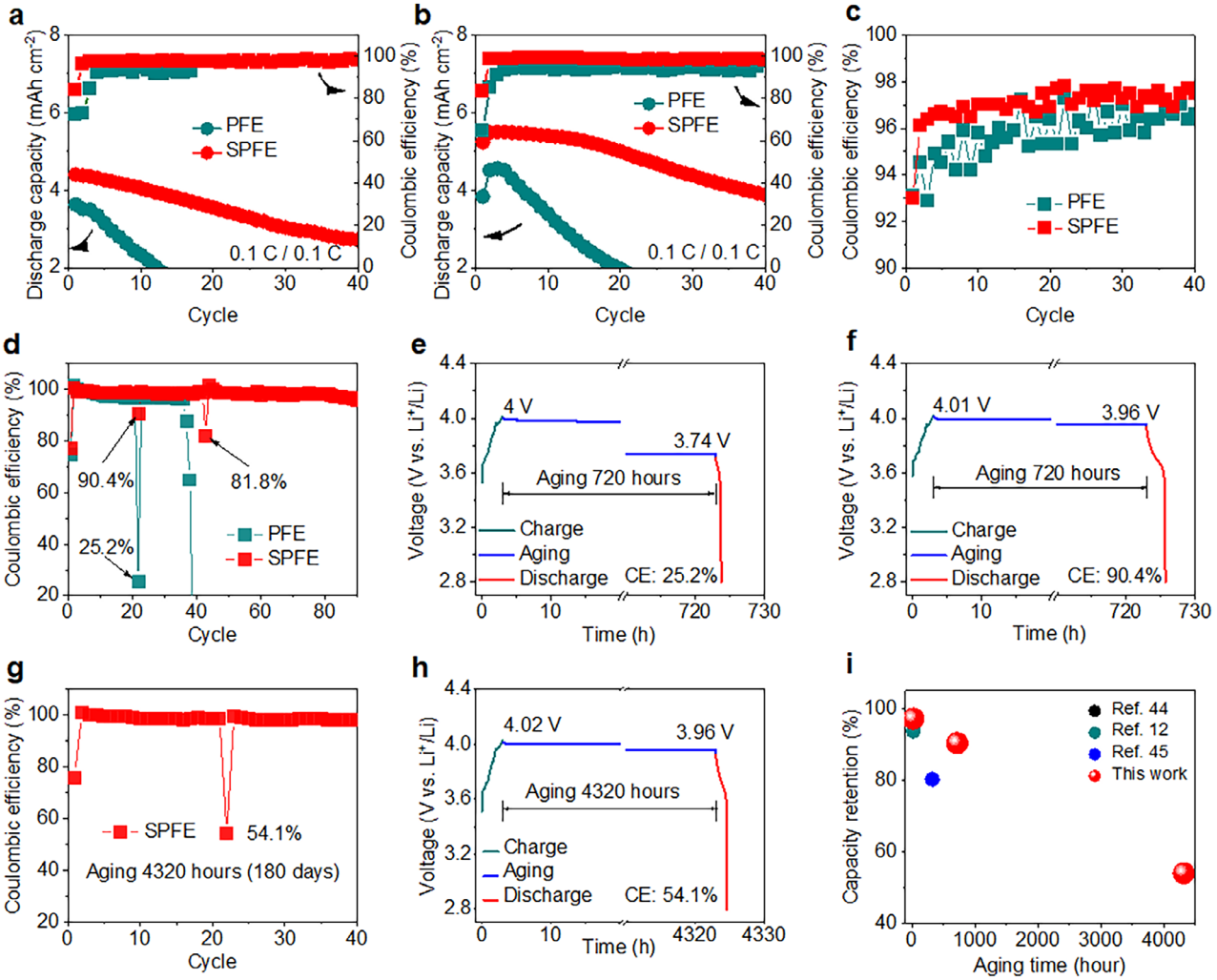

Figure 5. SPFE for ultralong life AFLMBs. a, b) Intermittent cycling and aging test results for the AFLMBs with NMC622 (28 mg cm^{-2}) and SCNMC811 (26 mg cm^{-2}) cathodes, respectively. c) Coulombic efficiencies for the intermittent cycling and aging test of Li | Cu half cells. d) 30 days calendar aging performance of AFLMBs (NMC622 (28 mg cm^{-2}) | Cu) charged through volcano current (3 h charge). Specifically, the 22nd and 43rd cycle were the aging cycles, where the AFLMBs were charged to ≈65% SoC first and then followed by remaining to open circuit-voltage (OCV) for 30 days. Then the cell was discharged to 2.8 V. Voltage-time curves for the calendar aging cycle (22nd) of AFLMBs (30 days) with e) PFE and f) SPFE electrolytes, respectively. g) 180 days calendar aging performance of AFLMBs with NMC622 (28 mg cm^{-2}) cathode. h) Voltage-time curves for the calendar aging cycle (22nd) of AFLMBs (180 days). i) Comparisons for the calendar aging performance of AFLMBs in present research with other reported researches.

180 days aging (Figure 5g,h), a record high value[6,29] (Figure 5i; Table S2, Supporting Information). The concept of SPFE, such as the combination of Li metal and $LiNO_3$ can stabilize PFE electrolyte under harsh conditions, can also be expanded for LIBs with graphite anode or silicon&graphite hybrid anode. For example, the LIBs with graphite anode which use PP/$LiNO_3$/PP separator can increase the CE of 68.1% for the cell use PP/PP separator to be 96% at the 10th cycle of intermittent cycling and aging test (Figure S36, Supporting Information), and the LIBs with silicon&graphite hybrid anode which use PP/$LiNO_3$/PP separator can increase the CE of 76.3% for the cell use PP/PP separator to be 94.7% at the 10th cycle of intermittent cycling and aging test (Figure S37, Supporting Information). To demonstrate the effectiveness of the present SPFE toward industry-scale production of AFLMBs, AF Li metal pouch cells (2Ah, 410 Wh kg^{-1}) were further fabricated under mostly DRF conditions. The cell with SPFE electrolyte can still deliver a capacity of 1.38 Ah and energy efficiency of 90.9% after 20 cycles, while the cell with PFE electrolyte can only deliver a capacity of 0.61 Ah and energy efficiency of 84% after 20 cycles (Figure S38, Supporting Information).

8. Conclusion

A stabilized P—F bond-based electrolyte (SPFE) is formulated to suppress the hydrolysis of $LiPF_6$. In this system, the quadruple reactions toward harmful species such as PF_5 and H_2O were designed, which include: I, the absorption between NO_3^- and PF_5; II, the absorption between NO_3^- and H_2O; III, the consumption of H_2O by nitrogenated organics through Nef reaction; IV, the absorption between aldehydes and H_2O. Among them, the latter two should be the keys for the co-existence of high content of water (3987.6 ppm) and $LiPF_6$-based electrolyte, where the

© 2025 Wiley-VCH GmbH

16163028, 2026, 9, Downloaded from https://advanced.onlinelibrary.wiley.com/doi/10.1002/adfm.202519229 by Tu Delft, Wiley Online Library on [09/02/2026]. See the Terms and Conditions (https://onlinelibrary.wiley.com/terms-and-conditions) on Wiley Online Library for rules of use; OA articles are governed by the applicable Creative Commons License

existence of Li metal will reduce the water content from 10 000 ppm to 3987.6 ppm, and the as-formed aldehydes can further restrain the degradation of $LiPF_6$-based electrolyte. With this SPFE, the corrosive decomposition of $LiPF_6$ has been largely restrained, resulting in an excellent stability of commercialized Li-ion pouch cells with electrolyte containing ultrahigh pristine water content of 10 000 ppm. This high moisture tolerance offers the mostly dry-room free (DRF) production of Li-ion pouch cells and next-generation high energy AFLMBs. This provides perspective on simplified manufacturing with decreased costs and improved stability upon cycling, aging, and recycling of lithium batteries.

9. Experimental Section

Materials: $LiPF_6$ particles and EC solids were provided by CAPCHEM. DEC solvent, FEC solvent, and $LiNO_3$ particles with purity over 99% were purchased from Aladdin. Li metal foil was purchased from China Energy Lithium Co., Ltd. NMP solvent (>98%) was purchased from Macklin. The commercial NMC622, SCNMC811, graphite and silicon&graphite hybrid powder, PVDF binder (PVDF5130, MW = 1200 000 Da, particle size: 100 µm, 99.5%), Super P (particle size: 40–50 nm, 99.5%), Al foil (thickness: 20 µm, 99.9%), Cu foil (thickness: 10 µm, 99.9%), separator (Celgard 2400) and coin cell components were purchased from Guangdong Canrd New Energy Technology Co., Ltd.

Ambient-Storage of Electrolyte: First, base electrolyte (1M $LiPF_6$ in EC/DEC (1/1, v/v) with 10 wt.% FEC, 10 mL), base electrolyte (10 mL) with 4 pieces Li metal foil (with diameter of 16 mm and thickness of 100 µm), base electrolyte (10 mL) with 1M $LiNO_3$-added and base electrolyte (10 mL) with both 4 pieces Li metal foil and 1M $LiNO_3$ were placed into different glass vial (20 mL), and they were denoted as Am, Am-Li, Am-L and Am-Li-L, respectively. Then these electrolytes were stored 90 days in ambient conditions with a temperature ranging from 15 to 30 °C and humidity ranging from 40% to 70%. After 60 days or 90 days of ambient storage, 2 mL of electrolyte from all four samples (Am, Am-Li, Am-L, and Am-Li-L) was pipetted from the storage vial in the glovebox for the pH test, water content test, NMR test, the redox cycling test of coin LIBs, and the calendar aging test of AFLMBs. The remaining samples would be kept for further storage in ambient conditions.

To further test the ambient-storage performance of water containing SPFE, 1 wt.% (10 000 ppm) of deionized water was injected into the four vials of newly prepared base electrolyte (20 mL) in ambient conditions. Then, these electrolytes were transferred into glovebox, with nothing added (H_2O-0d), with 6 pieces of Li metal foil (with diameter of 16 mm and thickness of 100 µm) added (H_2O-Li-0d), with 4M $LiNO_3$ added (H_2O-L-0d), and with both 6 pieces of Li foil and 4M $LiNO_3$ added (H_2O-Li-L-0d), respectively, and then they were transferred to ambient conditions. These electrolytes were ambient-stored for 15 days in ambient conditions with temperature ranging from 22 to 27 °C and humidity ranging from 60% to 70%. It was worth noting that the Li metal in H_2O-Li-0d and H_2O-Li-L-0d samples will be gradually corroded by H_2O. Therefore, the corroded Li metal (6 pieces) in these two samples will be replaced by fresh Li metal (6 pieces) every 5 days. After 15 days of ambient storage, 0.3 mL of electrolyte from all these samples (H_2O-Am-15d, H_2O-Am-Li-15d, H_2O-Am-L-15d, and H_2O-Am-Li-L-15d) was withdrawn from the storage vial in the glovebox for water content testing. Then these electrolytes were employed for Li-ion pouch cell making (2 Ah, 200 Wh kg^{-1}).

Preparation of Anodes, Cathodes, and Separators: The commercial Cu foil with a thickness of 10 µm was punched into slices of 16 mm in diameter, and then they were immersed in dehydrated alcohol for 30 min of ultrasonic processing. Afterward, they were dried in a vacuum oven at 60 °C for 12 h. The as-obtained Cu slices were then transferred to a glovebox (H_2O<0.1 ppm, O_2<0.1 ppm) for further usage.

The high loading $LiNi_{0.6}Mn_{0.2}Co_{0.2}O_2$ (NMC622, 28 or 11 mg cm^{-2}), single crystal $LiNi_{0.8}Mn_{0.1}Co_{0.1}O_2$ (SCNMC811, 26 mg cm^{-2}) cathodes, graphite anode (G, 6 mg cm^{-2}) and silicon&graphite hybrid anode (Si&G, 3 mg cm^{-2}) were prepared via slurry-coating method. Typically, the pre-dried active material (NMC622, SCNMC811 and graphite), super P and PVDF were mixed in a mass ratio of 8:1:1. After grinding in a mortar, mixing with NMP and 6 h of stirring in a beaker, the as-formed slurries were blade-coated on Al foil with thickness of 20 µm (NMC622 and SCNMC811) or Cu foil with thickness of 10 µm (graphite and silicon&graphite). Upon evaporation of NMP in an oven at 80 °C, the Al supported cathodes were punched into slices of 12 mm in diameter, while the graphite coated Cu foil was punched into slices of 14 mm in diameter. Upon weighing and further drying in a vacuum oven at 60 °C for 12 h, these slices were transferred to the glovebox for further usage. Polypropylene (PP, Celgard 2400) with a diameter of 19 mm was used as the separator. The punched PP slices were washed with dehydrated alcohol first, and then they were dried in a vacuum oven at 60 °C for 12 h and transferred to the glovebox for further usage.

Coin Cell Assembly: The coin Li ion batteries (LIBs) were fabricated by matching high loading NMC622 cathodes (11 mg cm^{-2}) with Cu supported graphite anodes (6 mg cm^{-2}) or Cu supported silicon and graphite anodes (3 mg cm^{-2}) directly. To test the cycling and aging performances of anode-free LMBs (AFLMBs) with the ambient-stored electrolyte, the NMC622 cathodes (11 mg cm^{-2}) were matched with Cu slices directly. The ambient-stored electrolytes (60 or 90 days) were injected into the LIBs and anode-free LMBs directly in a glovebox, and one piece of PP membrane was used as the separator.

To quantify the corrosion resistance of SPFE in AFLMBs, the newly prepared electrolyte (1M $LiPF_6$ in EC/DEC (1/1, v/v) with 10 wt.% FEC) was used as a reference. The NMC622 cathodes (28 mg cm^{-2}) and SCNMC811 cathodes (26 mg cm^{-2}) were matched with Cu slices directly to test the intermittent aging and long-term aging performances of AFLMBs. The newly prepared electrolytes were injected into AFLMBs directly in a glovebox, and two pieces of PP membrane (PP/PP, PFE) or two pieces of PP membrane intercalated with $LiNO_3$ particles[25] (PP/$LiNO_3$/PP, SPFE) were used as the separator. In this research, 60 µL of electrolyte was used for the coin cell test.

Dry Room Preparation of Pouch Cells: The preparation of 2 Ah (200 Wh kg^{-1}) Li-ion battery with different water content was carried out in the dry room (with a dew point of ≈−40 °C) of Guangdong Graphene Innovation Center. For the cathode preparation, the dried NMC811 particles (Guangdong Canrd New Energy Technology) were mixed with PVDF, Super P and carbon nanotubes (CNTs) at mass ratio of 95:3:1.8:0.2. After mixing with NMP to form a homogeneous slurry, it was coated on Al foil (with thickness of 16 µm, Guangdong Canrd New Energy Technology) double-sided with an areal-loading of 30 mg cm^{-2}. After oven drying at 80 °C in a dry room (with a dew point of −50 °C) for 12 h, the coatings were sliced into NMC811 cathode (56 mm × 80 mm). For the anode preparation, the dried graphite particles obtained from Xiangfenghua Technology (TN-19) were mixed with PVDF, Super P, and carbon nanotubes (CNTs, Guangdong Canrd New Energy Technology) at a mass ratio of 95:3:1.8:0.2. After mixing with NMP, forming a homogeneous slurry, it was coated on Cu foil (with a thickness of 9 µm, Guangdong Canrd New Energy Technology) double-sided with an areal-loading of 11 mg cm^{-2}. After oven drying at 80 °C in a dry room (with a dew point of −50 °C) for 12 h, the coatings were sliced into Graphite anode (59 mm × 83 mm). Then the above cathodes (9 pieces) and anodes (10 pieces, eight double-sided and two single-sided) were stacked with a PP membrane. Upon packaging with Al-plastic film and injected with different electrolyte (3 g Ah^{-1}, the upper liquid layer after equilibrium between added $LiNO_3$ particles and Li metal foils), the un-activated Li-ion pouch cells were obtained. The N/P ratio for the pouch cell was 1.17, which was based on the actual capacity of anode (320 mAh g^{-1}) and cathode (200 mAh g^{-1}). Before the ex-factory test, these cells were first charged at 0.1 C current (1 C = 2 A) to 4.3 V and then further discharged to 3.0 V.

Mostly Dry Room Free (DRF) Preparation of Pouch Cells: The preparation of pouch cells under mostly dry room free (DRF) conditions was carried out in ambient conditions (with temperature ranging from 25 to 28 °C and humidity ranging from 55% to 75%.) directly. Typically, the parameters of cathodes, anodes, and the separator were the same as those of pouch cells prepared in dry room conditions. After stacking the cathodes, separator, and anodes, the obtained cells were packaged with Al-plastic film, and

© 2025 Wiley-VCH GmbH

16163028, 2026, 9, Downloaded from https://advanced.onlinelibrary.wiley.com/doi/10.1002/adfm.202519229 by Tu Delft, Wiley Online Library on [09/02/2026]. See the Terms and Conditions (https://onlinelibrary.wiley.com/terms-and-conditions) on Wiley Online Library for rules of use; OA articles are governed by the applicable Creative Commons License

then they were dried in a vacuum oven at 80 °C for 24 h. The dried cells were then transferred to a glovebox (H_2O<0.1 ppm, O_2<0.1 ppm) to fill with electrolyte. For the cell with PFE electrolyte, the base electrolyte (1M $LiPF_6$ in EC/DEC (1/1, v/v) with 10wt.% FEC) was added directly into it. For the cell with SPFE electrolyte, the PFE electrolyte with dispersed $LiNO_3$ particles (0.2 M) was prepared and then injected into the pouch cell first. Afterward, four pieces of Li metal foil (with a diameter of 16 mm and a thickness of 100 µm) were placed inside the pouch cell (without contacting with either the anode or the cathode). After 24 h of calendar aging, the four Li metal foils were taken out, and the pouch cell with SPFE electrolyte was obtained. For cell activation in a dry room, the pouch cells fabricated under ambient conditions were first charged at 0.1 C current (1 C = 2 A) to 4.3 V and then discharged to 3.0 V. Afterward, the gas bag of these cells was cut to release the gases produced, if any, before these cells were completely sealed.

Electrochemical Test: For the coin LIBs, the cells were charged to 4.3 V at 0.5 mA cm^{-2} (based on the area of cathode) and then discharged to 2.8V at 0.5 mA cm^{-2} first. Then these cells were cycled at 1 mA cm^{-2} in between 4.3 and 2.8 V. For the cycling and calendar aging performance of the coin AFLMBs (0.5 mA cm^{-2}) with different ambient-stored electrolytes, after the first cycle, these AFLMBs were charged to 4.3 V and then they were held at this open circuit voltage (OCV) for calendar aging. After 10 days, these AFLMBs were discharged to 2.8 V, and then it was further cycled in between 4.3 and 2.8 V. For the cycling performance of Li-ion pouch cell, the activated pouch cell was charged/discharged at 0.5 C current (1 C = 2 A) in between 4.3 and 2.8 V. For the cycling performance of AF Li metal pouch cell, the activated pouch cell was charged/discharged at 0.25 C current (1 C = 2 A) in between 4.3 and 2.8 V.

For the aging one-day test, the coin AFLMBs with NMC622 cathode (28 mg cm^{-2}) or SCNMC811 cathode (26 mg cm^{-2}) were charged to 4.3 V first. After that, the cells were held at this OCV for 24 h, and then it was discharged to 2.8 V and followed by the repeatedly intermittent charge-aging-discharge processes. For the long-term aging test of AFLMBs with NMC622 cathode (28 mg cm^{-2}) or SCNMC811 cathode (26 mg cm^{-2}), the as-prepared AFLMBs were charged with constant current or volcano current with a capacity of 3mAh cm^{-2} (the state of charge (SoC) was ≈65–70%), then they were discharged to 2.8 V. After being cycled 21 times, they were charged with the previous protocol, and then held at this OCV for 720 h (30 days) or 4320 h (180 days) before discharging to 2.8 V. The same procedure would be carried out in the 43th cycle (30 days of aging). All these cells were cycled at 25 °C.

Characterization: X-ray photoelectron spectroscopy (XPS) was adopted to explore the chemical information of disassembled electrodes. A PHI5000 VersaProbe II XPS with Al Kα irradiation (1486.6 eV) was employed. Scanning electron microscopy (SEM) was utilized to characterize the morphologies of the newly deposited Li metal in AFLMBs (to 4.3 V), and its corroded morphologies after being held at OCV for 48 h. The facility for SEM characterization was a cold field scanning electron microscope (SU8010, HITACHI) operated at 5 kV. Typically, to test the morphologies and XPS spectra for the charged anode before and after aging, the NMC622 cathode with a mass loading of 11 mg cm^{-2} was used to package AFLMBs. The SEI component and 3D distribution were obtained by time-of-flight secondary ion mass spectrometry (ToF-SIMS, PHI nanoTOF II, 30 keV, 2 nA) in a 200 µm (length) × 200 µm (width) region on the Li metal surface in Am-Li-L-60d electrolyte. The electrochemical impedance spectroscopy (EIS) measurements were conducted on a VMP3 electrochemical workstation (Bio Logic Science Instruments) over the frequency range of 10 kHz to 10 MHz with a disturbance amplitude of 10 mV.

Solution NMR: The ambient-stored electrolyte (0.2 mL) was mixed with 0.6 mL of Chloroform (CCl_3D)-d (with 0.03% V/V TMS) for 5 min. The solution was then transferred to an airtight NMR tube fitted with a plastic tap. 1D ^1H, ^{19}F, and ^{31}P NMR spectra were recorded on a Bruker AVANCE III HD 400MHz spectrometer using a BBO probe. ^1H spectra were internally referenced to TMS at 0 ppm (δ ^1H); ^{19}F and ^{31}P spectra were internally referenced to $LiPF_6$ at −74.5 ppm (δ ^{19}F) and −145.0 ppm (δ ^{31}P).

Density Functional Theory (DFT) Calculations: Based on the density functional theory (DFT), the Gaussian 16 and Gauss View 6.0 software were used to carry out all the calculations in this work. Typically, the B3LYP/6-311++G(d, p) basis set level and the ground state method were selected to optimize the molecular structure, and the basis set superposition error (BSSE) scale was set as 1.0 in the meantime.[30] In addition, the Solvation Model based on Density (SMD) model was used to treat the solvent effects.[31] To simplify the calculation process, the solvent system of $LiPF_6$-based carbonate electrolyte (1M $LiPF_6$ in EC/DEC (1/1, v/v) with 10 wt.% FEC) is treated as EC/DEC/FEC (5/5/1, v/v/v), where the ε_{EC} = 89.8, ε_{DEC} = 2.8, ε_{FEC} = 78.4[20] or 102.9.[21] Therefore, the dielectric constant for the electrolyte should be 49.21818 (ε_{FEC} = 78.4) and 51.44545 (ε_{FEC} = 102.9).

The Gibbs free energy (ΔG) of each reaction was calculated according to Equations (1) and (2):

$$\Delta G = E + G_{(corr)} \quad (1)$$

$$\Delta G_{dec.(AB)} = \Delta G_A + \Delta G_B - \Delta G_{AB} \quad (2)$$

where ΔG is the Gibbs free energy for the group, E is the zero-point energy of the group at the M05-2X/6-31G(d) level, $G_{(corr)}$ is the thermal corrected free energy of the group at the B3LYP/6-311++G(d, p) level, $\Delta G_{dec.(AB)}$ is the Gibbs free energy for the decomposition reaction of group AB into group A and group B, ΔG_A, ΔG_B and ΔG_{AB} are the Gibbs free energies of group A, B, and AB, respectively.

Supporting Information

Supporting Information is available from the Wiley Online Library or from the author.

Acknowledgements

Chen acknowledges the financial support from the National Natural Science Foundation of China and Research Grants Council of Hong Kong joint research program (N_CityU549/22), B.H. Li would like to acknowledge the support from the National Natural Science Foundation of China (No. 52261160384, 51872157, 52072208).

Conflict of Interest

The authors declare no conflict of interest.

Author Contributions

Y.L. and Y.T. contributed equally to this work. Y.L., B.L. and G.C. conceived and designed this project. B.L. and G.C. directed the project. Y.L. performed the electrode preparation and material characterizations, conducted the NMR tests, carried out the electrochemical measurements and battery tests, wrote the first draft and implemented the revisions. Y.T. carried out the DFT calculations. All authors discussed and analyzed the data. M.W., B.L. and G.C. revised the manuscript.

Data Availability Statement

The data that support the findings of this study are available from the corresponding author upon reasonable request.

Keywords

10 000 ppm, dry-room free cell, humidity tolerance, P—F bond, restrained corrosion

© 2025 Wiley-VCH GmbH

16163028, 2026, 9, Downloaded from https://advanced.onlinelibrary.wiley.com/doi/10.1002/adfm.202519229 by Tu Delft, Wiley Online Library on [09/02/2026]. See the Terms and Conditions (https://onlinelibrary.wiley.com/terms-and-conditions) on Wiley Online Library for rules of use; OA articles are governed by the applicable Creative Commons License

Received: July 29, 2025
Published online: August 19, 2025

[1] a) R. Fong, U. von Sacken, J. R. Dahn, *J. Electrochem. Soc.* **1990**, *137*, 2009; b) J. L. G. C. Nanjundiah, L. A. Dominey, V. R. Koch, *J. Electrochem. Soc.* **1988**, *135*, 2914; c) J. Yamaura, Y. Ozaki, A. Morita, A. Ohta, *J. Power Sources* **1993**, *43*, 233.
[2] a) M. S. Whittingham, *Science* **1976**, *192*, 1126; b) K. Mizushima, P. C. Jones, P. J. Wiseman, J. B. Goodenough, *Mater. Res. Bull.* **1980**, *15*, 783; c) J. J. Auborn, Y. L. Barberio, *J. Electrochem. Soc.* **1987**, *134*, 638.
[3] a) L. Sheng, K. Yang, J. Chen, D. Zhu, L. Wang, J. Wang, Y. Tang, H. Xu, X. He, *Adv. Mater.* **2023**, *35*, 2212292; b) F. Huttner, W. Haselrieder, A. Kwade, *Energy Technol.* **2020**, *8*, 1900245.
[4] a) G. Gachot, P. Ribière, D. Mathiron, S. Grugeon, M. Armand, J.-B. Leriche, S. Pilard, S. Laruelle, *Analy. Chem.* **2011**, *83*, 478; b) Y. Yu, P. Karayaylali, Y. Katayama, L. Giordano, M. Gauthier, F. Maglia, R. Jung, I. Lund, Y. Shao-Horn, *J. Phys. Chem. C* **2018**, *122*, 27368; c) J. Langdon, A. Manthiram, *Adv. Funct. Mater.* **2021**, *31*, 2010267; d) J. C. Hestenes, R. May, J. T. Sadowski, N. Munich, L. E. Marbella, *Chem. Mater.* **2022**, *34*, 232.
[5] X. Liu, D. Ren, H. Hsu, X. Feng, G.-L. Xu, M. Zhuang, H. Gao, L. Lu, X. Han, Z. Chu, J. Li, X. He, K. Amine, M. Ouyang, *Joule* **2018**, *2*, 2047.
[6] D. T. Boyle, W. Huang, H. Wang, Y. Li, H. Chen, Z. Yu, W. Zhang, Z. Bao, Y. Cui, *Nat. Energy* **2021**, *6*, 487.
[7] B. Niu, Z. Xu, J. Xiao, Y. Qin, *Chem. Rev.* **2023**, *123*, 8718.
[8] a) K. Kim, I. Park, S.-Y. Ha, Y. Kim, M.-H. Woo, M.-H. Jeong, W. C. Shin, M. Ue, S. Y. Hong, N.-S. Choi, *Electrochim. Acta.* **2017**, *225*, 358; b) M. Stich, M. Göttlinger, M. Kurniawan, U. Schmidt, A. Bund, *J. Phys. Chem. C* **2018**, *122*, 8836.
[9] a) S. E. Sloop, J. B. Kerr, K. Kinoshita, *J. Power Sources* **2003**, *119–121*, 330; b) C. L. Campion, W. Li, B. L. Lucht, *J. Electrochem. Soc.* **2005**, *152*, A2327; c) S. Wilken, M. Treskow, J. Scheers, P. Johansson, P. Jacobsson, *R.S.C. Adv.* **2013**, *3*, 16359.
[10] J. Henschel, F. Horsthemke, Y. P. Stenzel, M. Evertz, S. Girod, C. Lürenbaum, K. Kösters, S. Wiemers-Meyer, M. Winter, S. Nowak, *J. Power Sources* **2020**, *447*, 227370.
[11] X. Sun, H. S. Lee, X. Q. Yang, J. McBreen, *Electrochem. Solid-State Lett.* **2002**, *5*, A248.
[12] C.-K. Kim, D.-S. Shin, K.-E. Kim, K. Shin, J.-J. Woo, S. Kim, S. Y. Hong, N.-S. Choi, *Chem. Electro. Chem.* **2016**, *3*, 913.
[13] A. S. Wotango, W.-N. Su, E. G. Leggesse, A. M. Haregewoin, M.-H. Lin, T. A. Zegeye, J.-H. Cheng, B.-J. Hwang, *ACS Appl. Mater. Interfaces* **2017**, *9*, 2410.
[14] C. Xu, S. Renault, M. Ebadi, Z. Wang, E. Björklund, D. Guyomard, D. Brandell, K. Edström, T. Gustafsson, *Chem. Mater.* **2017**, *29*, 2254.
[15] M. Stich, N. Pandey, A. Bund, *J. Power Sources* **2017**, *364*, 84.
[16] W. E. Noland, *Chem. Rev.* **1955**, *55*, 137.
[17] Q. Gu, M. Wang, Y. Liu, Y. Deng, L. Wang, J. Gao, *ACS Appl. Mater. Interfaces* **2022**, *14*, 4759.
[18] J.-G. Han, K. Kim, Y. Lee, N.-S. Choi, *Adv. Mater.* **2019**, *31*, 1804822.
[19] X. Zhang, Y. Wang, Z. Ouyang, S. Wang, X. Zhao, Q. Xu, B. Yuan, X. Yue, Z. Liang, S. Geng, S. Tang, H. Sun, *Adv. Energy Mater.* **2024**, *14*, 2303048.
[20] A. Jänes, T. Thomberg, J. Eskusson, E. Lust, *ECS Trans.* **2014**, *58*, 71.
[21] M. Puget, V. Shcherbakov, S. Denisov, P. Moreau, J.-P. Dognon, M. Mostafavi, S. L.e Caër, *Chem. A Eur. J.* **2021**, *27*, 8185.
[22] F. Duffner, N. Kronemeyer, Tc, J. L., M. Winter, R. Schmuch, *Nat. Energy* **2021**, *6*, 123.
[23] a) J. C. Burns, N. N. Sinha, G. Jain, H. Ye, C. M. VanElzen, E. Scott, A. Xiao, W. M. Lamanna, J. R. Dahn, *J. Electrochem. Soc.* **2013**, *160*, A2281; b) L.-Q. Zheng, S.-J. Li, H.-J. Lin, Y.-Y. Miao, L. Zhu, Z.-J. Zhang, *Rus. J. Electrochem* **2014**, *50*, 904; c) W. Liu, H. Cai, D. Liu, R. Hua, H. Gao, R. Zhang, H. Tang, J. Li, D. Qu, *Int. J. Energy Res.* **2022**, *46*, 7988; d) Z. Chang, Y. Qiao, H. Deng, H. Yang, P. He, H. Zhou, *Energy Environ. Sci.* **2020**, *13*, 1197.
[24] D. Lin, Y. Liu, Y. Li, Y. Li, A. Pei, J. Xie, W. Huang, Y. Cui, *Nat. Chem.* **2019**, *11*, 382.
[25] Y. Liu, X. Qin, D. Zhou, H. Xia, S. Zhang, G. Chen, F. Kang, B. Li, *Energy Storage Mater.* **2020**, *24*, 229.
[26] a) Q. Shi, Y. Zhong, M. Wu, H. Wang, H. Wang, *Sci.* **2018**, *115*, 5676; b) Y. Liu, D. Lin, Y. Li, G. Chen, A. Pei, O. Nix, Y. Li, Y. Cui, *Nat. Commun.* **2018**, *9*, 3656.
[27] C.-T. Yang, Y. Qi, *Chem. Mater.* **2021**, *33*, 2814.
[28] a) R. Jung, F. Linsenmann, R. Thomas, J. Wandt, S. Solchenbach, F. Maglia, C. Stinner, M. Tromp, H. A. Gasteiger, *J. Electrochem. Soc.* **2019**, *166*, A378; b) H. Shin, Y. K. Lee, W. Lu, *J. Power Sources* **2022**, *528*, 231223; c) E. Björklund, C. Xu, W. M. Dose, C. G. Sole, P. K. Thakur, T.-L. Lee, M. F. L. De Volder, C. P. Grey, R. S. Weatherup, *Chem. Mater.* **2022**, *34*, 2034.
[29] a) P. Liang, H. Sun, C.-L. Huang, G. Zhu, H.-C. Tai, J. Li, F. Wang, Y. Wang, C.-J. Huang, S.-K. Jiang, M.-C. Lin, Y.-Y. Li, B.-J. Hwang, C.-A. Wang, H. Dai, *Adv. Mater.* **2022**, *34*, 2207361; b) Y. Gao, T. Rojas, K. Wang, S. Liu, D. Wang, T. Chen, H. Wang, A. T. Ngo, D. Wang, *Nat. Energy* **2020**, *5*, 534.
[30] D. O. Kashinski, G. M. Chase, R. G. Nelson, O. E. Di Nallo, A. N. Scales, D. L. VanderLey, E. F. C. Byrd, *J. Phys. Chem. A* **2017**, *121*, 2265.
[31] J. Ho, A. Klamt, M. L. Coote, *J. Phys. Chem. A* **2010**, *114*, 13442.

© 2025 Wiley-VCH GmbH

16163028, 2026, 9, Downloaded from https://advanced.onlinelibrary.wiley.com/doi/10.1002/adfm.202519229 by Tu Delft, Wiley Online Library on [09/02/2026]. See the Terms and Conditions (https://onlinelibrary.wiley.com/terms-and-conditions) on Wiley Online Library for rules of use; OA articles are governed by the applicable Creative Commons License